Biosensors and Bioelectronics 255 (2024) 116211

Contents lists available at ScienceDirect

Biosensors and Bioelectronics

journal homepage: www.elsevier.com/locate/bios

Peptide-based biosensing approaches for targeting breast cancer-derived exosomes

Rafael da Fonseca Alves [a,b,c], Arnau Pallarès-Rusiñol [a,b], Rosanna Rossi [a,b], Merce Martí [a], Emilia Rezende Vaz [d], Thaise Gonçalves de Araújo [d], Maria Del Pilar Taboada Sotomayor [c], Maria Isabel Pividori [a,b,*]

[a] Biosensing and Bioanalysis Group, Institute of Biotechnology and Biomedicine, Universitat Autònoma de Barcelona, Spain
[b] Grup de Sensors i Biosensors, Departament de Química, Universitat Autònoma de Barcelona, Bellaterra, Spain
[c] Institute of Chemistry, State University of São Paulo (UNESP), Brazil
[d] Institute of Biotechnology (IBTEC), Federal University of Uberlandia (UFU), Uberlandia, MG, Brazil

ARTICLE INFO

Keywords:
Exosomes
Mitovesicles
Peptide-based biosensors
Phage display
Magnetic separation
Proteomic analysis

ABSTRACT

Exosomes are nanovesicles present in all the biological fluids, making them attractive as non-invasive biomarkers for diseases like cancer, among many others. However, exosomes are complex to separate and detect, requiring comprehensive molecular characterization for their routine use in diagnostics. This study explores the use of peptides as cost-effective and stable alternatives to antibodies for exosome binding. To achieve that, phage display technology was employed to select peptides with high specificity for target molecules in exosomes. Specifically, a selected peptide was evaluated for its ability to selectively bind breast cancer-derived exosomes. Proteomic analysis identified 38 protein candidates targeted by the peptide on exosome membranes. The binding of the peptide to breast cancer-derived exosomes was successfully demonstrated by flow cytometry and magneto-actuated immunoassays. Furthermore, an electrochemical biosensor was also tested for breast cancer-derived exosome detection and quantification. The peptide demonstrated effective binding to exosomes from aggressive cancer cell lines, offering promising results in terms of specificity and recovery. This research shows potential for developing rapid, accessible diagnostic tools for breast cancer, especially in low-resource healthcare settings.

1. Introduction

Exosomes are small extracellular vesicles of nanometric dimensions (Gurung et al., 2021; Théry et al., 2018) released by most cells into biological fluids, including blood (Johnsen et al., 2019), serum, plasma, urine, among others. (Cappello et al., 2017). Their main biological functions are related to intercellular communication and the transport of active biomolecules, proteins, and nucleic acids to host cells (Mathieu et al., 2019; Valadi et al., 2007). These features, including their availability in body fluids and the biologically active cargo, make them good candidates as biomarkers for diseases such as cancer (Weng et al., 2021; Yu et al., 2022). The composition of these vesicles is complex, including receptors, enzymes, lipids, mRNA, miRNA and other types of proteins and nucleic acids. Their endosomal biogenesis pathway (Gurung et al., 2021; Mathieu et al., 2019) provides exosomes with their distinct biological signature derived from their mother cells. Therefore, exhaustive molecular characterization studies are required before implementing them in *in vitro* diagnostic tests. Regarding membrane biomarkers, tetraspanins (CD9, CD63 and CD81) are described as hallmark biomarkers (Andreu and Yáñez-Mó, 2014; Théry et al., 2018). However, the size, molecular complexity and variability of exosomes makes extremely difficult to find specific biomarkers for targeting them for downstream analysis, including either separation or detection (Yáñez-Mó et al., 2015). Peptides obtained by phage-display are currently being considered as alternative bioreceptor to antibodies, due to their lower cost and increased stability. Since the earlier reports on Phage Display (Smith, 1985), this technique is considered a powerful screening technology to look for new peptides and proteins with high affinity and specificity for a target of interest (Pande et al., 2010; Zambrano-Mila et al., 2020). Phage Display has also proved to be a

* Corresponding author. Biosensing and Bioanalysis Group, Institute of Biotechnology and Biomedicine, Universitat Autònoma de Barcelona, Spain.
E-mail address: isabel.pividori@uab.cat (M.I. Pividori).

https://doi.org/10.1016/j.bios.2024.116211
Received 9 January 2024; Received in revised form 4 March 2024; Accepted 11 March 2024
Available online 19 March 2024

valuable strategy for the development of bioreceptors for biosensing applications (Escobar et al., 2023; Peltomaa et al., 2019; Xu et al., 2021) as well as for the characterization of exosomes (Maisano et al., 2022), among many other applications. In this work, the study of a peptide selected by phage display for the selective binding of breast cancer exosomes derived from MCF-7, MDA-MB231 and SKBR3 cell lines is reported. The engineered peptide was previously designed by co-authors of this work, targeting MCF-7 cells, obtaining promising results with electrochemical biosensing of human sera from healthy and breast cancer patients (da Fonseca Alves et al., 2022). First, a proteomic study using MCF-7 exosomes was used to identify the candidate proteins targeted by the engineered peptide on the surface of exosomes membranes. The binding of the biotin-C3 peptide to cancer-derived exosomes from the three breast cancer cell lines was further assessed by bead-based flow cytometry (Pallares-Rusiñol et al., 2023a; Volgers et al., 2017) using immobilized exosome on magnetic particles (Moura et al., 2020a). Then, a magneto-actuated immunoassay was designed and tested using the engineered peptide (modified with biotin) as detection probe, while capturing the exosomes with biologically modified MPs against CD63 tetraspanin receptors. Finally, an electrochemical biosensor was designed for the detection and quantification of cancer-derived exosomes spiked in human serum, with outstanding analytical performance and recovery values. In all instances, exosomes derived from MRC-5 fibroblasts cell line as non-tumorigenic negative control were included, in order to provide for a clearer differentiation between the specific results observed in cancer cells and the broader responses within the tumor environment. The format of this biosensor is unprecedented, as it specifically targets extracellular vesicles, making it suitable for the analysis of liquid biopsies. The innovative aspects of the strategy presented here integrate key components aiming to achieve simplification while maintaining outstanding analytical performance for the detection of exosomes. Specifically, a peptide obtained through phage display is introduced as alternative bioreceptor for exosome biosensing, offering cost-effective and stable option. By combining magnetic separation techniques with electrochemical biosensors based on a peptide for labelling, significant improvement in biosensing technology is achieved, enhancing sensitivity and specificity in exosome detection. The use of a cartridge for magnetic actuation, washing and readout minimizes user intervention, improving system ease of use and reproducibility. Furthermore, a remarkable improvement in the limit of detection is achieved using peptide-based labeling strategies, promising higher diagnostic accuracy and reliability. The results obtained in this work, place peptides obtained by phage-display as a good alternative to antibodies as biorecognition elements in various bioanalytical assays as well as in biosensing devices with very promising analytical features.

2. Materials and methods

2.1. Reagents and instrumentation

Based on the expression frequency in biopanning and the results obtained from the phage display, the best candidate peptide named biotin-C3 was synthesized with >95% purity (Gen Script Biotech) with the sequence Acetyl-**SAMPPFYTAPGW**GGGSAETVESCL-Lys-biotin. Additionally, some modifications were made by acetylating the N-terminal end to facilitate interaction with the target ligand. After the active fraction of 12 aa, a spacer sequence of other further 12 aa was introduced to mimic, as closely as possible, the conformation expressed in the phage. Finally, a lysine residue was added to link a biotin molecule to the peptide. All further materials and reagents were of analytical grade as described in detail in the S1 (Supp. Data), as well as the instrumentation.

2.2. Cell culturing, exosome isolation and purification

Breast cancer cell lines MCF-7 (ER and PR positive, ref- HTB-22), MDA-MB231 (TN, ref. HTB-26) and SKBr3 (HER2 positive, ref. HTB-30) and the fibroblast lineage MRC-5 (used as a non-tumorigenic negative control, ref. CCL-171) were obtained from the American Type Culture Collection (ATCC). Cell population expansion was performed from 5×10^6 cells in a T-175 flask containing 35 mL of Dulbecco's modified Eagle's Glutamax medium (DMEM), except for the MRC-5 strain, for which DMEM-α medium was used. Media were supplemented with 10% exosome-depleted fetal bovine serum (FBS) and 100 U mL^{-1} of penicillin-streptomycin. Temperature was maintained at 37 °C in a humidified and concentrated CO_2 atmosphere (5 %). Once the cells reached approximately 95 % confluence in the T-175 flask, the culture supernatant was removed and stored at −20 °C until exosomes isolation, following protocol detailed in S2 (Supp data) and Fig. S2 therein.

2.3. LC–MS/MS and proteomic analysis

Proteins from MCF-7 strain were extracted and quantified according to the procedure described in S3.1 (Supp. data). After extraction, the proteins were isolated and preconcentrated by magnetic separation. To achieve that, the biotin-C3 peptide was immobilized on streptavidin-modified magnetic particles for protein capture, following the procedure described in S3.2 (Supp. data). The same procedure was performed, except for biotin-C3 peptide addition, to obtain a blank sample for comparison. The samples were frozen at −80 °C and subsequently analyzed by mass spectrometry. 125 ng of blank and 500 ng of MCF-7 respectively were loaded onto the liquid chromatographic system. LC column temperature was set at 40 °C, and separation was performed at a flow rate of 0.5 μL min^{-1} in a 120-min acetonitrile gradient ranging from 3% to 40% (solvent A: 0.1% formic acid, solvent B: 0.1% formic acid in acetonitrile). The resulting digested peptides were analyzed with mass spectrometer (MS) operated in positive ionization mode with a spray voltage of 1.8 kV. The spectrometric analysis was performed in a data dependent mode with a full scan acquisition followed by 10 MS/MS scans of the 10 most intense signals detected in the MS scan from the global list. The full MS (range 400–1600 m/z) was acquired in the Orbitrap with a resolution of 60.000. LC-MS/MS spectra were searched using SEQUEST (Proteome Discoverer v1.4, ThermoFisher). All parameters for data acquisition and bioinformatic analysis are described in S3.2 (Supp data) (Yan et al., 2020).

2.4. Characterization of the exosomes derived from breast cancer cell lines

The size distribution and concentration of exosomes were measured by nanoparticle tracking analysis (NTA). The morphology was analyzed by cryogenic transmission electron microscopy (Cryo-TEM). The total protein concentration of exosomes samples was estimated by a BCA protein assay kit. All the procedures are described in S4.1 (Supp data). Bead-based flow cytometry was also used to characterize the ability of biotin-C3 peptide to recognize targets present on the membrane of exosomes derived from breast cancer cell lines MCF-7, MDA-MB231, and SKBr3. Specifically, the behavior and differentiation of exosomes directly immobilized on MPs (as shown on Figure S4.1), or captured by the tetraspanins CD63, CD9, and CD81 receptors (as shown on Figures S4.2, S4.3 and S4.4, respectively) were evaluated (following protocol detailed in S4.2 Supp data).

2.5. Magneto-actuated immunoassay

Microtiter plates (96 wells) were used for the magneto-activated immunoassay. Exosomes were captured using anti-CD63-modified MPs (antiCD63-MPs), containing 1×10^6 antiCD63-MPs per well and 100 μL of exosomes at concentrations ranging from 150 to 4.8×10^6 exosomes μL^{-1}, for 30 min with gentle agitation at 25 °C. After incubation, the solution was discarded, and the plate was washed three times with 200

μL per well of 1× PBS solution containing 0.5% BSA (PBS-BSA). Then, the biotin-C3 peptide (2.0 μg per well) diluted in PBS-BSA solution was added and incubated for 1 h at 37 °C. The complex was labeled with strep-polyHRP (100 μL, 10 ng mL^{-1}) iluted in PBS-BSA and incubated for 1 h at 37 °C. Following the incubation period, the wells were washed three times with PBS-BSA, and then 100 μL of Pierce™ TMB substrate kit was added per well and incubated for 30 min at room temperature. The reaction was stopped by adding 2.0 M H_2SO_4. The absorbance was measured on a microplate reader at 450 nm. The magnetic separation process was performed after each incubation or washing step by positioning a 96-well magnetic plate separator under the microtiter plate until the pellets formed in the lower corner, followed by the separation of the supernatant.

2.6. Electrochemical biosensor for the detection of exosomes in serum

For the calibration plot, exosomes (100 μL) with concentrations ranging from 150 to 4.8 × 10^6 exosomes μL^{-1} were incubated with anti-CD63 MPs (containing 1 × 10^6 anti-CD63 MPs per well) for 30 min under gentle shaking at 25 °C. This was followed by three washes with PBS-BSA and the addition of biotin-C3 peptide (2.0 μg per well). The complex was labeled with strep-polyHRP (100 μL, 10 ng mL^{-1}) diluted in PBS-BSA and incubated for 1 h at 37 °C.

Subsequently, the content was transferred to a cartridge (Bio-Ecloclion SL, Spain) containing a screen-printed electrode (DRP-C110 screen-printed carbon electrodes from Dropsens, Spain). Further details related the electrochemical readout is detailed in S5 (Supp. data). Alongside characterization by NTA, CryoTEM, bead-based flow cytometry, and proteomics analysis, standard recovery assessments were conducted for the magneto-actuated immunoassay and the electrochemical biosensing. The study involved spiking known amounts (quantified by NTA) of purified exosomes from breast cancer cell lines (MCF-7, MDA-MB231, and SKBr3) into depleted human serum (centrifuged at 20,000×*g*) to assess the efficiency of exosome recovery and potential losses during sample preparation and analysis. In all instances, human serum without exosome addition was used as a control.

2.7. Statistical analysis

Data from analytical curves were fitted using a non-linear regression (four parameter logistic equation) in GraphPad Prism 10 software (San Diego, USA). Limits of detection (LODs) were calculated by interpolation of mean plus 3-fold SD of negatives control sample currents.

3. Results and discussion

3.1. Proteomics analysis

A dysregulation in extracellular vesicle (EV) biogenesis has been reported in cancer, leading to an increased release and alteration of exosome components in blood and serum. (Jabalee et al., 2018; Xavier et al., 2020). In a previous study, the biotin-C3 peptide was successfully used to differentiate serum from patients with breast cancer to benign breast disease (da Fonseca Alves et al., 2022). The proteomics study was carried on showed 365 protein groups with some affinity with the biotin-C3 peptide, excluding those shared with the control, and the results are summarized in Figure S3.1 (Supp. data). 38 protein exclusively located in plasma and organelle membranes were selected for further analysis, as they could be the potential targets of biotin-C3 peptide on the membrane of breast cancer exosomes, as shown in Figure S3.1, panel A (Supp. data). Interestingly, 27 out of 38 protein groups showed some interaction by STRING analysis (Figure S3.1, panel B, Supp. data) and classification analysis of protein families showed they are all involved in pathways related with cancer. Among the 38 identified proteins (listed in Table S3, Supp. data), data suggesting a connection to breast cancer was found for 16 of them, as detailed in S3.3 (Supp data). Among the identified proteins, 11 had a mitochondrial origin.

Mitovesicles, small extracellular vesicles that transport mitochondrial components, are currently under investigation for their potential roles in cancer progression, metastasis, and drug resistance, positioning them as a focal point in oncological research (Zhou et al., 2023). For instance, exosomes from breast cancer cells promote invasion, induce myeloid differentiation, suppress the immune response, and confer drug resistance through mitochondrial delivery (Zhou et al., 2023). Mitochondrial proteins can constitute up to 10 % of the total protein content in exosomes (Choi et al., 2013). The altered metabolism of tumor cells, particularly in aggressive cancers as triple-negative breast cancer, leads to an accumulation of mitochondrial proteins. Moreover, mitochondrial proteins are absent in samples from healthy controls but present in those derived from cancer tumors (Jang et al., 2019). Considering the role of mitochondria in cellular metabolic regulation (Cassim et al., 2020; Martínez-Reyes and Chandel, 2021; McAndrews and Kalluri, 2019), the results suggest the Biotin-C3 peptide as a potential marker of tumor formation, progression, response to therapy and/or metastasis (Cassim et al., 2020; Vasan et al., 2020). To summarize, the Biotin-C3 peptide demonstrates specificity by targeting these distinct vesicle subpopulations. The presence of tumor-specific mitochondrial proteins in vesicles, absent in healthy controls, further underscores the significance of the Biotin-C3 peptide in cancer-related investigations as biomarker.

3.2. Molecular docking of protein-protein binding

To investigate the interaction between the sequenced proteins and the biotin-C3 peptide, molecular docking simulation using the online server HDOCK was performed (Yan et al., 2020). Their calculated binding energies and confidence scores are presented in Table S3 while the docking results for the interaction between the biotin-C3 peptide and the 38 proteins identified are summarized in Figure S3.2 (Supp. data). This analysis reinforces the data of proteomic analysis, indicating a possible interaction between the biotin-C3 peptide and the 38 identified proteins. Notably, the subunit c of cytochrome oxidase (O00483) and the subunit of the mitochondrial cytochrome *b-c*1 Rieske complex (P47985), both present in the inner membrane of mitochondria, as well as extended synaptotagmin-1 (Q9BSJ8), present in the membrane of the endoplasmic reticulum, showed higher scores. The most interested candidates of protein/biotin-C3 peptide binding are detailed discussed in S3.4 (Supp. data).

3.3. Characterization of the exosomes derived from breast cancer cell lines

The NTA analysis of exosomes derived from breast cancer cell lines revealed a similar size distribution, as depicted in Fig. 1, panels A to D, for MCF-7, MDA-MB231, SKBr3, and MRC-5 (as non-tumorigenic negative control), respectively. The size distribution histogram of MCF-7 exosomes showed a distinct peak at 145 nm and a less intense peak at 215 nm. For MDA-MB231 exosomes, two peaks were observed at 130 and 185 nm, respectively, along with a smaller peak at 295 nm corresponding to small aggregates. For SKBr3 exosomes, NTA analysis revealed a clear peak at 145 nm and another smaller peak at 255 nm, while MRC-5 exosomes exhibited a peak at 125 nm and another smaller peak at 285 nm.

The observed variations in the size distribution histograms of MCF-7, MDA-MB231, SKBr3, and MRC-5 cell lines highlight differences in the populations of exosomes released by each cell line, likely influenced by factors such as cellular origin or physiological state. However, despite these differences, consistent peaks between 100 and 200 nm confirm the presence of nano-sized extracellular vesicles, commonly identified as exosomes. This confirms the robustness of the extracellular vesicle isolation method. Besides size distribution, particle concentration was also estimated using NTA, being the corresponding concentration 8.09 × 10^{10} particle·mL^{-1} (SD 1.93 × 10^{10}) for MCF-7; 1.14 × 10^{11}

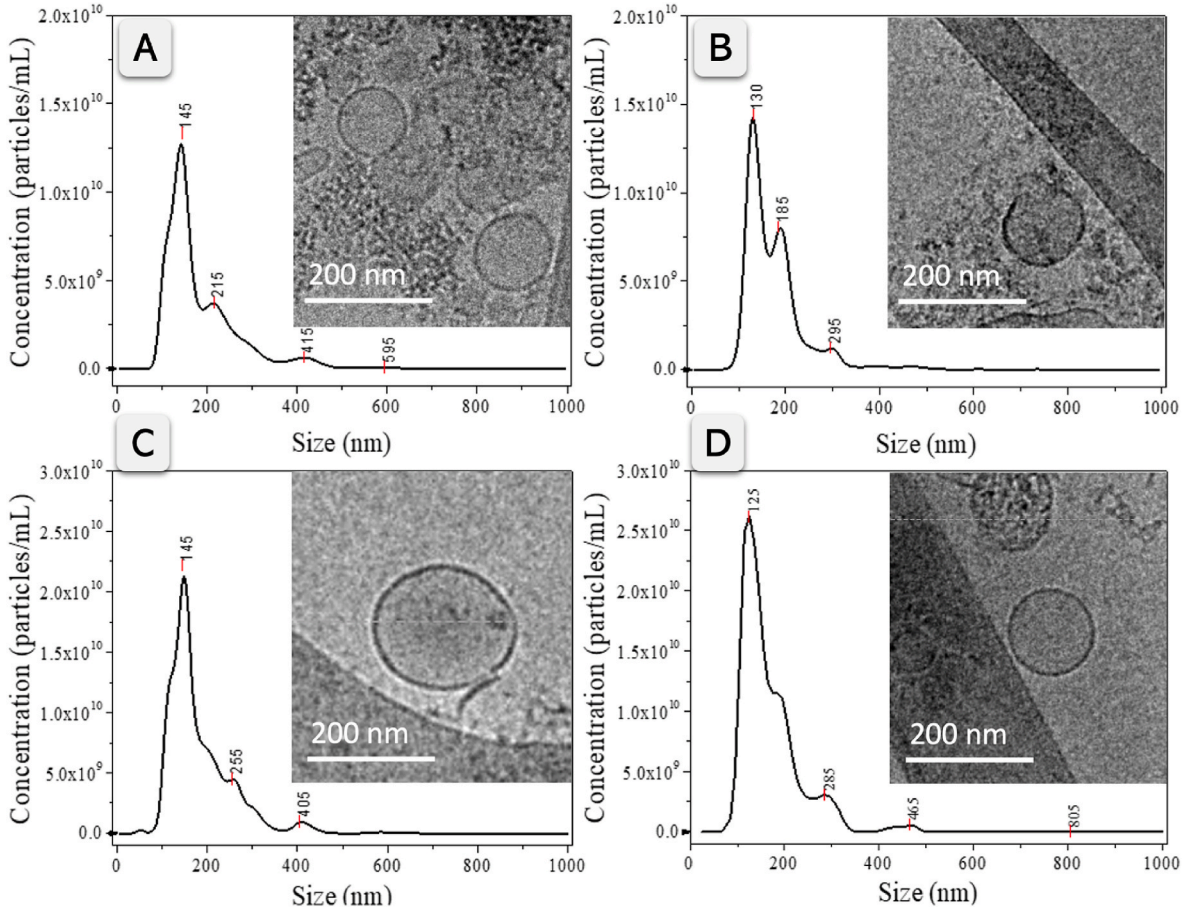

Fig. 1. Characterization by NTA and Cryo-TEM of purified exosomes-derived from (A) MCF-7, (B) MDA-MB231, (C) SKBr3, and (D) fibroblast cell line MRC-5 as non-tumorigenic negative control. The NTA characterization analyzed raw data videos in triplicate for 60 s with 25 frames per second, and the laser unit temperature was set to 24.8 °C. Cryo-TEM images were obtained at an acceleration voltage of 200 kV.

particle·mL^{-1} (SD 3.00 × 10^{9}) for MDA-MB231; 1.88 × 10^{11} particle·mL^{-1} (SD 1.40 × 10^{10}) for SKBr3, and finally, 2.28 × 10^{11} particle·mL^{-1} (SD 8.00 × 10^{9}) for MRC-5. Exosome samples were also imaged with cryogenic transmission electron microscopy to evaluated particle size and integrity of the vesicles, as shown in Fig. 1 as insets for each cell line sample.

To evaluate the recognition capacity of the biotin-C3 peptide and the presence of ligand targets in exosomes derived from various cell lines, including MCF-7, MDA-MB231, SKBr3, and MRC-5, bead-based flow cytometry assays were conducted. First, exosomes immobilized directly on magnetic particles were labeled with the biotin-C3 peptide, as described in detail in S4.2 (Supp. data) and previously described by the group (Moura et al., 2020a). Figure S4.1 shows that the biotin-C3 peptide recognized targets present in exosomes and presented a differential profile among cell lines, with positive labeling of 99.0% in exosomes derived from MFC-7, 96.5% in exosomes derived from MDA-MB231, 51.4% in exosomes derived from SKBr3, and only 1.9% in exosomes derived from MRC-5. The results are also summarized in Fig. 2 as a heat map. Therefore, the biotin-C3 peptide recognizes targets present in exosomes derived from breast cancer cells and, more relevantly, with greater intensity in MCF7 and MDA-MB231 cell lines. Although molecularly distinct, MCF7 is luminal and positive for ER and MDA-MB231 is triple negative, both are considered more aggressive and with greater metastatic potential compared to SKBr-3 (Saez et al., 1989; Yordanova and Hassan, 2022). Regarding exosome production, it is known that tumor cells with higher metastatic potential tend to produce more exosomes, which may be related to tumor dissemination to other organs. (Huang et al., 2022).

Thus, the results suggest that there are mechanisms involved in the metastatic process of molecularly distinct subtypes of breast cancer cells. Furthermore, the specificity of the peptide to label only exosomes derived from the most aggressive cells and not fibroblasts is interesting since fibroblasts are a type of cell present in the tumor microenvironment (Li et al., 2021).

Tetraspanins are integral membrane proteins that play crucial roles in supporting protein structure and anchoring to cellular membranes. Exosomes express tetraspanins CD9, CD63, and CD81 significantly, which are commonly used as exosome universal biomarkers and can influence their formation and composition (Hemler, 2003). Therefore, further experiments were performed with magnetic particles modified with antibodies against the tetraspanins in order to capture, separate and preconcentrate exosomes, as described in detail in S4.2 (Supp. data). The results are shown in Figures S4.2–S4.4 in Supp data for anti-CD63, anti-CD9 and anti-CD81, respectively, and the results are also summarized in Fig. 2 as a heat map. Biotin-C3 peptide differentially recognized targets present in exosomes depending on the antibody used in the capture and the cell line. For exosomes captured with anti-CD63, a positive labeling of 92.4 % was obtained for exosomes derived from MFC-7, 95.0 % for exosomes derived from MDA-MB231, 0.4 % for exosomes derived from SKBr3, and 0.03 % for exosomes derived from MRC-5 (Figure S4.2). For exosomes captured with anti-CD9, a positive labeling of 75.5% was obtained for exosomes derived from MFC-7, 46.9% for exosomes derived from MDA-MB231, 10.2% for exosomes derived from SKBr3, and 3.5% for exosomes derived from MRC-5 (Figure S4.3). Finally, for exosomes captured with anti-CD81, a positive labeling of 74.1 % was obtained for exosomes derived from MFC-7,

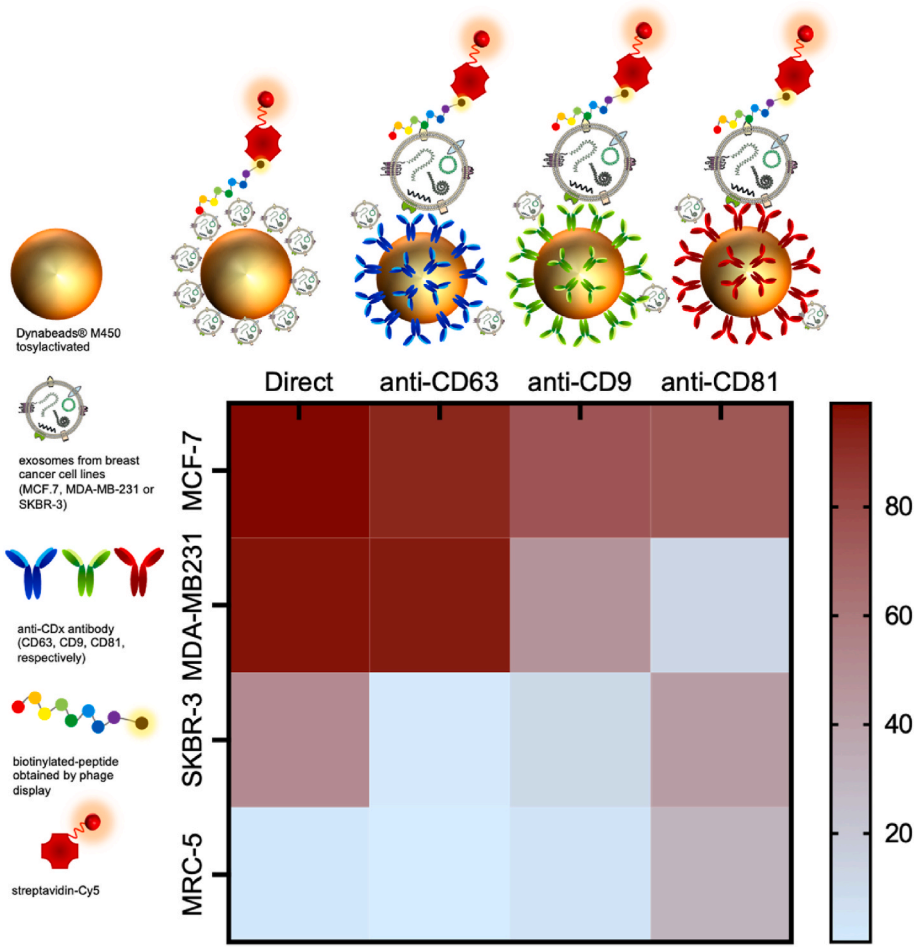

Fig. 2. Summary of the results obtained by bead-based flow cytometry for characterization of breast cancer-derived exosomes, indicating the percentage of positive labeling with biotin-C3 peptide/streptavidin-Cy5. MRC-5 fibroblast cell line as non-tumorigenic negative control was also added.

11.4 % for exosomes derived from MDA-MB231, 41.5 % for exosomes derived from SKBr3, and 30.4 % for exosomes derived from MRC-5 (Figure S4.4). Two successful immunomagnetic separation approaches were performed: direct and sandwich. In the direct approach, exosomes were directly immobilized onto magnetic particles and labeled with biotin-C3 peptide. In the sandwich approach, exosomes were previously captured by antibody-modified magnetic particles and labeled with biotin-C3 peptide (Fig. 2). It is important to highlight that the direct approach is only feasible for expression profiling using purified exosomes. In real matrices, immobilization of antibodies that bind to these vesicles, such as CD9, CD63, and CD81 tetraspanins, has been shown to be applicable to biological fluids. (Moura et al., 2020b) since the exosomes must be previously separated for further labelling. In this instance, direct immobilization of purified exosomes presented a similar profile to those captured by anti-CD63, being this tetraspanin an excellent candidate in combination with the peptide. Accordingly, anti-CD63 was used in this work for quantification approaches including magneto immunoassay and electrochemical biosensing in further experiments.

The results of the sandwich approach demonstrated that the biotin-C3 peptide labeled poorer exosomes derived from the SKBr3 lineage, indicating the peptide ability to identify a specific subpopulation of EVs. These findings offer guidance for selecting the best magnetic immunoseparation approach for analyzing exosomes in different cell lines. The specific labeling of biotin-C3 peptide may be useful for identifying exosomes derived from different cell subtypes, which may have important implications for using these vesicles as biomarkers in cancer diagnosis and treatment (Khushman et al., 2017). In fact, tetraspanin-bearing EVs, especially CD9 and CD81, with low expression of CD63, are mainly derived from the plasma membrane, while those expressing CD63 with little CD9 are formed in internal compartments and characterized as exosomes (Mathieu et al., 2019). The study evaluating the efficacy of biotin-C3 peptide in labeling exosomes using antibody-modified magnetic particles with anti-CD9, anti-CD63, and anti-CD81 antibodies demonstrated that the approach using anti-CD63 antibody showed greater similarity with the labeling profile obtained by direct capture of exosomes derived from MCF-7 and MDA-MB231 cell lines. These results directly corroborate the findings in protein sequencing analyses, where many of the candidate targets binding to the biotin-C3 peptide are membrane proteins from cellular organelles such as mitochondria and endoplasmic reticulum. Additionally, the experiment confirmed the efficacy of using anti-CD63 antibody in immunomagnetic separation of exosomes, making it the appropriate choice for the development of the bioanalytical approaches presented in further studies.

3.4. Magneto-actuated immunoassay

A magneto-actuated ELISA with optical redout was first studied to detect exosomes derived from breast cancer cell lines using the biotin-C3 peptide. Fig. 3, panel A shows a scheme of the magnetic capture and colorimetric reaction process, while Fig. 3, panel B presents the calibration plot for exosomes derived from MCF-7, MDA-MB231, SKBr3 breast cancer cell lines, and the MRC-5 fibroblast cell line as non-tumorigenic negative control.The calibration plot was constructed for different exosome concentrations, ranging from 150 to 4.8 $\times$ 10^6

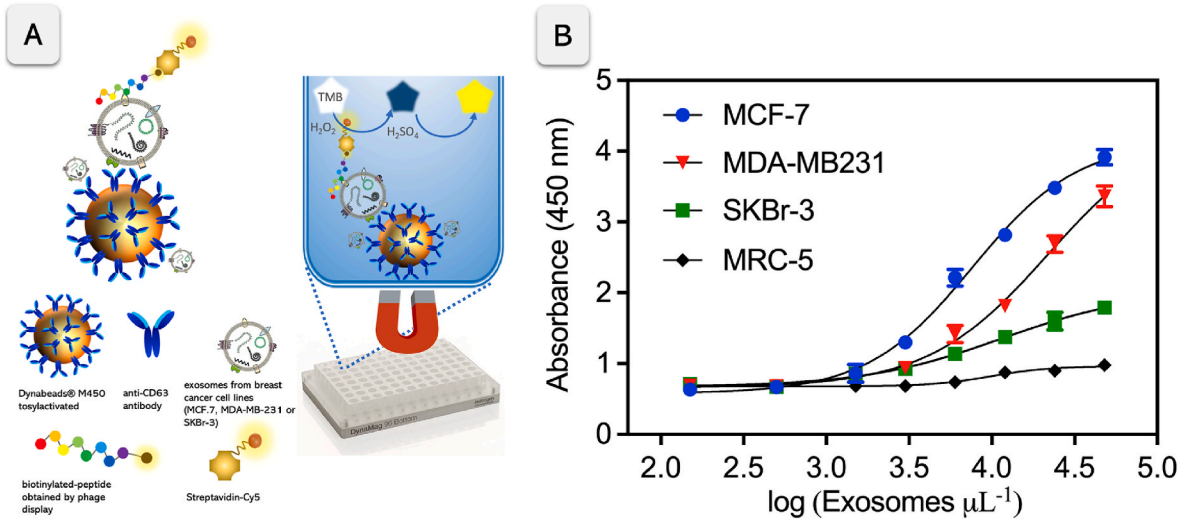

Fig. 3. Magneto-actuated immunoassay for the detection of exosomes derived from breast cancer cell lines MCF-7, MDA-MB231, SKBr3, and fibroblast cell line MRC-5 as non-tumorigenic negative control. (A) Schematic outline of the approach, involving the covalent immobilization of anti-CD63 on magnetic particles, followed by labeling with biotin-C3 peptide and streptavidin-polyHRP, and colorimetric reaction with TMB. (B) Calibration plots at 450 nm at exosome concentration ranging from 150 to 4.8 × 10^6 exosomes μL^{-1}, fitted using a non-linear regression (four-parameter logistic equation) (n = 3).

exosomes μL^{-1}. The absorbance values were fitted using a non-linear regression (four-parameter logistic equation). The limits of detection (LOD) were 330 exosomes μL^{-1} ($r^2 = 0.9928$), 388 exosomes μL^{-1} ($r^2 = 0.9904$), and 473 exosomes μL^{-1} ($r^2 = 0.9708$) for exosomes derived from MCF-7, MDA-MB231, and SKBr3 cell lines, respectively. These values represent an improvement by an order of 3, compared to previous studies (from 10^5 to 10^2 exosomes μL^{-1}) compared to other magneto-actuated immunoassay based on a similar principle for immuno-magnetic separation (IMS) but relaying on different principles to achieve the optical readout, including a second labeled antibody in a sandwich immunoassay format (Moura et al., 2020a).

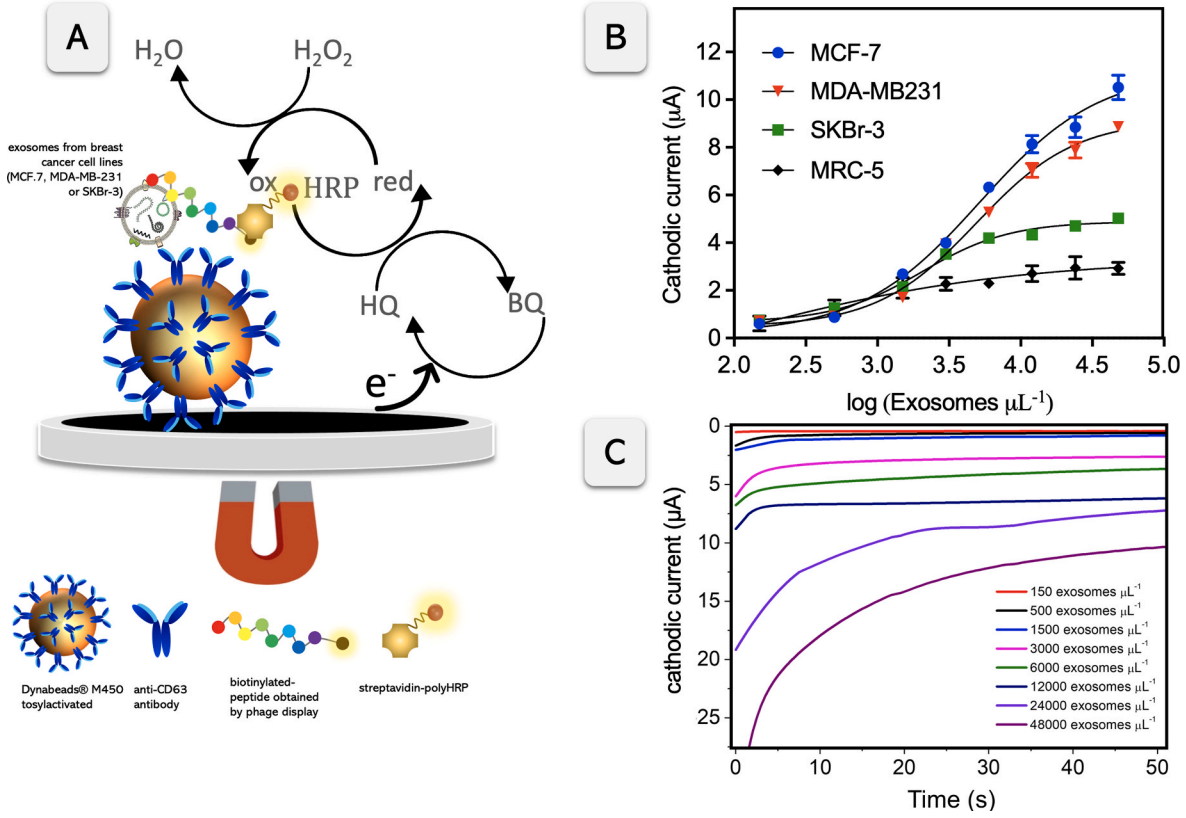

Fig. 4. Electrochemical biosensing for the detection of exosomes derived from breast cancer cell lines MCF7, MDA-MB231, SKBr3, and the fibroblast cell line MRC-5 as non-tumorigenic negative control. (A) Schematic outline of the approach, involving the covalent immobilization of anti-CD63 on magnetic particles, followed by labeling with biotin-C3 peptide and streptavidin-polyHRP, and electrochemical readout. (B) Calibration plots at exosome concentration ranging from 150 to 4.8 × 10^6 exosomes μL^{-1} (according to NTA counting), fitted using a non-linear regression (four-parameter logistic equation). The error bars show the standard deviation for n = 3. (C) Raw chronoamperograms for exosomes derived from the MCF-7 cell line ranging from 150 to 4.8 × 10^6 exosomes μL^{-1}.

Table 1
Analytical performance of the magneto-actuated immunoassay and the electrochemical biosensor of exosomes derived from breast cancer cell lines MCF7, MDA-MB231, SKBr3, captured by antiCD63-MPs and labeled with biotin-C3 peptide, and spiked on depleted human serum. n = 3.

Exosome-type	Exosomes μL^{-1}	Recovery (%) Electrochemical biosensor	RSD (%)	Recovery (%) Magneto-actuated immunoassay	RSD (%)
MCF7	6.0×10^3	111.9	3.2	108.8	9.4
	4.8×10^4	107.3	4.1	103.6	7.3
MDA-MB231	6.0×10^3	97.6	6.5	95.4	7.3
	4.8×10^4	111.1	8.8	105.9	8.9
SKBr3	6.0×10^3	93.9	6.1	91.2	8.9
	4.8×10^4	98.3	9.8	96.6	9.8

3.5. Electrochemical biosensor for the detection of exosomes in serum

The calibration plots for the detection of exosomes derived from different cancer cells lines (MCF-7, MDA-MB231, SKBr3, and fibroblast MRC-5 as negative control) are comparatively shown in Fig. 4, at a concentration ranging from 150 to 4.8×10^6 exosomes μL^{-1}.

The magnetic separation of exosomes based on anti-CD63, followed by electrochemical detection using the biotin-C3 peptide and streptavidin-polyHRP, is shown in Fig. 4, panel B. The adjusted signals obtained an LODs of 175 exosomes μL^{-1} ($r^2 = 0.9907$), 189 exosomes μL^{-1} ($r^2 = 0.9914$), and 262 exosomes μL^{-1} ($r^2 = 0.9809$) for exosomes derived from MCF-7, MDA-MB231, and SKBr3 cell lines, respectively, with the lowest LOD for the MCF-7 cell line, as expected. These values represent an improvement by an order of 3, compared to previous studies (from 10^5 to 10^2 exosomes μL^{-1}) compared to other immunosensors based on a similar principle for immunomagnetic separation (IMS) of the exosomes but relaying on different principles to achieve the electrochemical readout, including a second labeled antibody in a sandwich immunosensing format (Moura et al., 2020b). Remarkably, the LODs found were of the same order than the biosensors based on the intrinsic alkaline phosphatase enzyme activity in exosomes in a simplified analytical procedure (Moura et al., 2022). Also, in the electrochemical genosensing, based on exosomes isolation and preconcentration by IMS, followed by further double-tagging RT-PCR as a strategy to amplify the signal by using a common and the ubiquitous transcript GAPDH (Pallares-Rusiñol et al., 2023b). All this features are summarized in Table S6, Supp. data. This improvement can be clearly attributed to the biotin-C3 peptide in combination to streptavidin-polyHRP for labeling, in this instance to achieve the electrochemical readout, due to the smaller size compared to antibodies, which can be advantageous in terms of improved diffusion and binding kinetics in complex targets as is the case of the exosomes. Given the absence of a universally accepted gold standard for evaluating accuracy in exosome analysis, a standard recovery study of exosomes in depleted human serum was conducted. This aimed to validate the efficiency of exosome recovery through immunomagnetic separation and to evaluate potential losses during sample preparation and analysis. The results from the magneto-ELISA and magneto-actuated biosensor with electrochemical detection for the recovery study are presented in Table 1, demonstrating remarkable recovery values ranging from 91.2 to 111.9, as well as good reproducibility in human serum, especially in the case of the biosensing devices for the MCF-7 and MDA-MB231exosomes. The combination of modified MPs with anti-CD63, followed by detection based on a peptide selected by phage display and binding to breast cancer tumor protein ligands, provided promising results in terms of recovery and detection of exosomes in enriched serum matrix without the need for further sample treatment or dilution.

4. Conclusions

This study presents a biosensing device for breast cancer-derived exosomes, involving immunomagnetic separation with antiCD63 and electrochemical readout based on the biotin-C3 peptide. The LODs represented a three-fold improvement compared to previous studies, reaching values on the order of 175 exosomes μL^{-1}. The peptide obtained via phage display demonstrated efficacy in detecting exosomes through various methods, with enhanced LODs for aggressive cell lineages. A proteomic analysis identified 38 membrane proteins targeted by the biotin-C3 peptide, with 16 associated with breast cancer and 11 originating from mitochondria. Very promising results suggest that the Biotin-C3 peptide targets mitovesicles, highlighting its potential as a marker for tumor-related processes, particularly in breast cancer-derived extracellular vesicles. Peptides from phage display offer advantages over antibodies in biosensors due to their stability, cost-effectiveness, scalability, and reproducibility. The biotin-C3 peptide shows promise as a prognostic tool for patient monitoring, although further clinical validation is necessary. The design of the cartridge for the electrochemical readout is a user-friendly feature that minimizes the need for user intervention, contributing also to the ease of use and reproducibility of the system, and preventing pipetting and washing steps. The integration of electrochemical readout in a portable device operated by batteries enables on-site and point-of-care testing. All these features could have significant implications for real-world applications and are combined in a significant improvement in LOD. In conclusion, while this study has demonstrated the promising prognostic potential of the Biotin-C3 peptide in a biosensing device for detecting cancer-derived exosomes, further validation is necessary, including a clinical validation of the efficacy of this approach and assessing its impact on patient outcomes.

CRediT authorship contribution statement

Rafael da Fonseca Alves: Writing – original draft, Validation, Methodology, Investigation. **Arnau Pallarès-Rusiñol:** Writing – original draft, Methodology, Investigation. **Rosanna Rossi:** Writing – review & editing, Writing – original draft, Methodology, Investigation. **Merce Martí:** Supervision. **Emilia Rezende Vaz:** Supervision. **Thaise Gonçalves de Araújo:** Writing – original draft, Supervision, Resources. **Maria Del Pilar Taboada Sotomayor:** Writing – review & editing, Writing – original draft, Supervision, Resources. **Maria Isabel Pividori:** Writing – review & editing, Writing – original draft, Supervision, Funding acquisition, Conceptualization.

Declaration of competing interest

The authors declare that they have no known competing financial interests or personal relationships that could have appeared to influence the work reported in this paper.

Data availability

The datasets generated during the current study are available in the CORA RDR repository, https://dataverse.csuc.cat/.

Acknowledgment

This research was funded by the Ministry of Science, Innovation and Universities, Spain (Projects PID2019-106625RB-I00/AEI/10.13039/

501100011033, PID2022-136453OB-I00 and PDC2022-133363) and from Generalitat de Catalunya (2021SGR-00124). Also, São Paulo State Research Foundation - Brazil (FAPESP, grant #2019/10452-2 and grant #2021/12307-0), Coordination for the Improvement of Higher Education Personnel (CAPES), the National Council for Scientific and Technological Development (CNPq), and National Institute of Science and Technology in Theranostics and Nanobiotechnology – INCT – Teranano. Minas Gerais Research Foundation – Brazil (FAPEMIG, grant # APQ-00760-18 and grant REMITRIBIC RED-00031-21), the National Council for Scientific and Technological Development (CNPq – grant # 305328/2022-0). ICTS "NANBIOSIS" NTA analysis service of Institut de Ciència dels Materials de Barcelona, Service of Microscopy and Proteomics and Structural Biology Servicec of Universitat Autònoma de Barcelona are gratefully acknowledged.

Appendix A. Supplementary data

Supplementary data to this article can be found online at https://doi.org/10.1016/j.bios.2024.116211.

References

Andreu, Z., Yáñez-Mó, M., 2014. Front. Immunol. 5 https://doi.org/10.3389/fimmu.2014.00442.
Cappello, F., Logozzi, M., Campanella, C., Bavisotto, C.C., Marcilla, A., Properzi, F., Fais, S., 2017. Eur. J. Pharmaceut. Sci. 96, 93–98. https://doi.org/10.1016/J.EJPS.2016.09.010.
Cassim, S., Vučetić, M., Ždralević, M., Pouyssegur, J., 2020. Cancers 12 (5). https://doi.org/10.3390/CANCERS12051119.
Choi, D.S., Kim, D.K., Kim, Y.K., Gho, Y.S., 2013. Proteomics 13, 1554–1571. https://doi.org/10.1002/pmic.201200329.
da Fonseca Alves, R., Martins, I.C., Franco, D.L., Silva, A. das G., de Souza Santos, P., Goulart, L.R., Cristina de Paiva Maia, Y., Faria Silva, A.T., Gonçalves Araújo, T., Del Pilar Taboada Sotomayor, M., 2022. Biosens. Bioelectron. 205, 114081 https://doi.org/10.1016/j.bios.2022.114081.
Escobar, V., Scaramozzino, N., Vidic, J., Buhot, A., Mathey, R., Chaix, C., Hou, Y., 2023. Biosensors 13. https://doi.org/10.3390/bios13020258.
Gurung, S., Perocheau, D., Touramanidou, L., Baruteau, J., 2021. Cell Commun. Signal. 19, 1–19. https://doi.org/10.1186/s12964-021-00730-1.
Hemler, M.E., 2003. Annu. Rev. Cell Dev. Biol. 19, 397–422. https://doi.org/10.1146/annurev.cellbio.19.111301.153609.
Huang, S., Dong, M., Chen, Q., 2022. Metastasis. Int. J. Mol. Sci. 23, 13993 https://doi.org/10.3390/IJMS232213993.
Jabalee, J., Towle, R., Garnis, C., 2018. Cells 7. https://doi.org/10.3390/CELLS7080093.
Jang, S.C., Crescitelli, R., Cvjetkovic, A., Belgrano, V., Olofsson Bagge, R., Sundfeldt, K., Ochiya, T., Kalluri, R., Lötvall, J., 2019. J. Extracell. Vesicles 8 (1). https://doi.org/10.1080/20013078.2019.1635420.
Johnsen, K.B., Gudbergsson, J.M., Andresen, T.L., Simonsen, J.B., 2019. Biochim. Biophys. Acta Ver. Cancer 1871, 109–116. https://doi.org/10.1016/J.BBCAN.2018.11.006.
Khushman, M., Bhardwaj, A., Patel, G.K., Laurini, J.A., Roveda, K., Tan, M.C., Patton, M. C., Singh, S., Taylor, W., Singh, A.P., 2017. Pancreas 46, 782–788. https://doi.org/10.1097/MPA.0000000000000847.
Li, C., Teixeira, A.F., Zhu, H.J., ten Dijke, P., 2021. Mol. Cancer 20. https://doi.org/10.1186/S12943-021-01463-Y.
Maisano, D., Mimmi, S., Dattilo, V., Marino, F., Gentile, M., Vecchio, E., Fiume, G., Nisticò, N., Aloisio, A., De Santo, M.P., Desiderio, G., Musolino, V., Nucera, S., Sbrana, F., Andò, S., Ferrero, S., Morandi, A., Bertoni, F., Quinto, I., Iaccino, E., 2022. Nanoscale 14, 2998–3003. https://doi.org/10.1039/D1NR06804K.
Martínez-Reyes, I., Chandel, N.S., 2021. Nat. ver. Cancer 21 (10), 669–680. https://doi.org/10.1038/s41568-021-00378-6.
Mathieu, M., Martin-Jaular, L., Lavieu, G., Théry, C., 2019. Nat. Cell Biol. 21, 9–17. https://doi.org/10.1038/s41556-018-0250-9.
McAndrews, K.M., Kalluri, R., 2019. Mol. Cancer 18 (1), 1–11. https://doi.org/10.1186/S12943-019-0963-9.
Moura, S.L., Martín, C.G., Martí, M., Pividori, M.I., 2020a. Talanta 211, 120657. https://doi.org/10.1016/j.talanta.2019.120657.
Moura, S.L., Martín, C.G., Martí, M., Pividori, M.I., 2020b. Biosens. Bioelectron. 150, 111882 https://doi.org/10.1016/j.bios.2019.111882.
Moura, S.L., Pallares-Rusiñol, A., Sappia, L., Martí, M., Pividori, M.I., 2022. Biosens. Bioelectron. 198, 113826 https://doi.org/10.1016/j.bios.2021.113826.
Pallares-Rusiñol, A., Bernuz, M., Moura, S.L., Fernández-Senac, C., Rossi, R., Martí, M., Pividori, M.I., 2023a. Advances in exosome analysis. In: Adv. Clin. Chem. Academic Press Inc., pp. 69–117. https://doi.org/10.1016/bs.acc.2022.09.002
Pallares-Rusiñol, A., Moura, S.L., Martí, M., Pividori, M.I., 2023b. Anal. Chem. 95 (4), 2487–2495. https://doi.org/10.1021/acs.analchem.2c04773.
Pande, J., Szewczyk, M.M., Grover, A.K., 2010. Biotechnol. Adv. 28, 849–858. https://doi.org/10.1016/J.BIOTECHADV.2010.07.004.
Peltomaa, R., Benito-Peña, E., Barderas, R., Moreno-Bondi, M.C., 2019. ACS Omega 4, 11569–11580. https://doi.org/10.1021/ACSOMEGA.9B01206.
Saez, R.A., McGuire, W.L., Clark, G.M., 1989. Semin. Surg. Oncol. 5, 102–110. https://doi.org/10.1002/SSU.2980050206.
Smith, G.P., 1985. Science 228 (4705), 1315–1317. https://doi.org/10.1126/SCIENCE.4001944.
Théry, C., Witwer, K.W., Aikawa, E., et al., 2018. J. Extracell. Vesicles 7. https://doi.org/10.1080/20013078.2018.1535750.
Valadi, H., Ekström, K., Bossios, A., Sjöstrand, M., Lee, J.J., Lötvall, J.O., 2007. Nat. Cell Biol. 9, 654–659. https://doi.org/10.1038/ncb1596.
Vasan, K., Werner, M., Chandel, N.S., 2020. Cell Metabol. 32 (3), 341–352. https://doi.org/10.1016/J.CMET.2020.06.019.
Volgers, C., Benedikter, B.J., Grauls, G.E., Savelkoul, P.H.M., Stassen, F.R.M., 2017. Microbiol. Res. 200, 25–32. https://doi.org/10.1016/J.MICRES.2017.04.003.
Weng, J., Xiang, X., Ding, L., Li, A., Wong, -Ann, Zeng, Q., Sethi, G., Wang, L., Lee, S.C., Goh, B.C., 2021. Semin. Cancer Biol. 74, 105–120. https://doi.org/10.1016/j.semcancer.2021.05.011.
Xavier, C.P.R., Caires, H.R., Barbosa, M.A.G., Bergantim, R., Guimarães, J.E., Vasconcelos, M.H., 2020. Cells 9, 1141. https://doi.org/10.3390/CELLS9051141.
Xu, P., Ghosh, S., Gul, A.R., Bhamore, J.R., Park, J.P., Park, T.J., 2021. TrAC, Trends Anal. Chem. 137, 116229 https://doi.org/10.1016/j.trac.2021.116229.
Yan, Y., Tao, H., He, J., Huang, S.Y., 2020. Nat. Protoc. 15, 1829–1852. https://doi.org/10.1038/s41596-020-0312-x.
Yáñez-Mó, M., Siljander, P.R.-M., Andreu, Z., et al., 2015. J. Extracell. Vesicles 4, 27066. https://doi.org/10.3402/jev.v4.27066.
Yordanova, M., Hassan, S., 2022. Curr. Oncol. 29, 2008–2020. https://doi.org/10.3390/CURRONCOL29030163.
Yu, D., Li, Y., Wang, M., Gu, J., Xu, W., Cai, H., Fang, X., Zhang, X., 2022. Mol. Cancer 21, 1–33. https://doi.org/10.1186/s12943-022-01509-9.
Zambrano-Mila, M.S., Blacio, K.E.S., Vispo, N.S., 2020. Ther. Innov. Regul. Sci. 54, 308–317. https://doi.org/10.1007/s43441-019-00059-5.
Zhou, X., Liu, S., Lu, Y., Wan, M., Cheng, J., Liu, J., 2023. J. Extracell. Vesicles 12 (4), e12320. https://doi.org/10.1002/jev2.12320.